ELSEVIER

Journal of Physics and Chemistry of Solids 63 (2002) 833–841

JOURNAL OF PHYSICS AND CHEMISTRY OF SOLIDS

www.elsevier.com/locate/jpcs

Electronic structure calculations of lead chalcogenides PbS, PbSe, PbTe

Mohammed Lach-hab[a], Dimitrios A. Papaconstantopoulos[a,b,*], Michael J. Mehl[b]

[a]*School of Computational Sciences and Informatics, George Mason University, Fairfax, VA 22030-4444, USA*
[b]*Center for Computational Materials Science, Naval Research Laboratory, Washington, DC 20375, USA*

Received 7 August 2001; accepted 1 October 2001

Abstract

In this work, we have extended our study of the mechanical properties and the electronic structure of PbTe to include other Pb chalcogenide compounds (PbSe, PbS). The calculations were performed self-consistently using the scalar-relativistic full-potential linearized augmented plane wave method. Both the local density approximation (LDA) and the generalized gradient approximation (GGA) to density-functional theory were applied.

The equilibrium lattice constants and the bulk modulus of a number of structures (NaCl, CsCl, ZnS) were calculated as well as the elastic constants for the structures (NaCl, CsCl). The NaCl structure is found to be the most stable one among all the three phases considered. We have found that the GGA predicts the elastic constants in good agreement with experimental data.

Both the LDA and GGA were successful in predicting the location of the band gap at the *L* point of the Brillouin zone but they are inconclusive regarding the value of the band-gap width. To resolve the issue of the gap, we performed Slater–Koster (SK) tight-binding calculations, including the spin–orbit coupling in the SK Hamiltonian. The SK results that are based on our GGA calculations give the best agreement with experiment.

Results are reported for the pressure dependence of the energy gap of these compounds in the NaCl structure. The pressure variation of the energy gap indicates a transition to a metallic phase at high pressure. Band structure calculations in the CsCl structure show a metallic state for all compounds. The electronic band structure in the ZnS phase shows an indirect band gap at the *W* and *X* point of the Brillouin zone.

Keywords: A. Chalcogenides; D. Electronic structure; D. Elastic properties

1. Introduction

The small energy gap of lead chalcogenide (PbS, PbSe, PbTe) semiconductors is one of the most important properties leading to the great experimental interest in these materials. Because of their practical use in electronic devices these naturally occurring IV–VI semiconductors have received increased attention since the early experimental investigation of transistors [1] in 1951. The development of modern computers provided the computational resources which led to many theoretical studies of the electronic structure and the elastic properties of these materials.

Among band structure, investigations of the lead chalcogenide rock salt phase are those of Wei and Zunger [2] who employed the linearized augmented plane wave (LAPW) method [3,4] within the local density approximation (LDA) [5]. Earlier theoretical studies of the electronic structure of these materials were made by many groups, using a semi-empirical tight-binding (TB) method [6], augmented plane waves (APW) [7,8], the Green function method [9], orthogonalized plane waves [10], and the empirical-pseudopotential method [11–15]. These theoretical calculations identified a direct band gap at the *L* point of the Brillouin zone for all three lead chalcogenides.

In this work, we present LAPW calculations in both the LDA and the generalized gradient approximation (GGA) [16] to determine the elastic properties and the electronic

* Corresponding author. Address: Center for Computational Materials Science, Naval Research Laboratory, Washington, DC 20375, USA. Fax: +1-202-404-7546.

E-mail address: papacon@dave.nrl.navy.mil (D.A. Papaconstantopoulos).

0022-3697/02/$ - see front matter
PII: S0022-3697(01)00237-2

band structure of the lead chalcogenide compounds. Surprisingly, we find that the GGA overestimates the band gap for all three systems. Since Pb is a heavy element, we use a TB technique to investigate the behavior of the band gap with spin–orbit coupling. The organization of this paper is as follows. In Section 2, we present the computational procedure used in the LAPW method and the Slater–Koster (SK) fit approach by which we have introduced the spin–orbit interaction. In Section 3, our LAPW results for the band structures and the mechanical properties of the NaCl structure are presented, and we compare the LDA and GGA results to experimental and other theoretical data. We also describe the effect of spin–orbit coupling on the band gap, as deduced from our TB calculations. Finally, we conclude this work with a summary in Section 4.

2. The method

In the full potential LAPW method [3,4], we treat the core electrons in a full relativistic atomic-like calculation and the valence electrons in a scalar relativistic calculation [17] omitting the spin–orbit coupling. The valence electrons in the lead chalcogenide compounds correspond to the atomic configurations $d^{10}s^2p^2$ for lead (Pb) and s^2p^4 for the chalcogens (S, Se, Te).

We have used two methods for calculating the exchange and correlation potential energy: the LDA using the Hedin–Lundqvist parametrization [18] and the GGA using the Perdew–Wang formalism [16]. Our plane wave cutoff was such that $RK_{\max} = 9.5$ with muffin-tin (MT) radius $R = 2.5$ a.u. Special k-point sets were used with 85 k-points in the irreducible Brillouin zone. Within these approximations, we have calculated the total energy self-consistently to an accuracy of the order of 0.01 mRy. Our calculations of the total energy as a function of volume are fitted by least squares to the Birch [19] equation of state $E(V)$. With this procedure, we calculate the equilibrium volume V_0 and evaluate the bulk modulus at equilibrium using the equation:

$$B_0 = \left(V \frac{\partial^2 E}{\partial V^2} \right)_{V_0} \tag{1}$$

To calculate the elastic constants, we adopt the same scheme for deformation as those used by Mehl et al. [20,21]. Two kinds of deformations on the cubic crystal were used for the study; a monoclinic strain conserving volume which determines C_{44}, and an orthorhombic strain conserving volume that determines $C_{11} - C_{12}$. Using this scheme the elastic constants are defined as the second derivatives of the energy with respect to deformation parameters. The three independent elastic constants needed for a cubic crystal are given as follows:

$$C_{11} - C_{12} = \frac{1}{V} \frac{\partial^2 E}{\partial X^2}, \qquad C_{44} = \frac{2}{V} \frac{\partial^2 E}{\partial X^2}, \qquad C_{11} + 2C_{12} = 3B, \tag{2}$$

where X is the strain, and E is the total energy. The cubic structure can be stable only if the stability criteria [22,23]

$$C_{11} - C_{12} > 0, \qquad C_{44} > 0, \qquad B_0 > 0, \tag{3}$$

are satisfied.

For the band structure calculations of the lead chalcogenide semiconductors, we first used the general potential LAPW method in the scalar-relativistic approximation, omitting the spin–orbit interactions. However, since we are dealing with atoms which have large atomic numbers, the inclusion of spin–orbit coupling is essential for an accurate evaluation of the band structure. The spin–orbit effect can be easily treated within the SK [24] formalism of TB theory.

We applied an SK interpolation method [25] to fit the energy bands for PbS, PbSe, and PbTe. In the fit, we used an orthogonal basis set of s and p orbitals for each atom in the unit cell following the procedure summarized in Refs. [25,26]. We used as adjustable parameters 32 three-center interaction integrals, including both first and second neighbors. These parameters were determined by a nonlinear least-squres fit to both LDA and GGA results for the seven lowest bands. The rms fitting error was less than 8 mRy for all bands. The resulting SK parameters for our GGA results are given in Table 1. The SK parameters for PbTe given in Ref. [26] correspond to LDA results. These parameters were determined by a nonlinear least-squares fit to the MT APW results. We then introduce the spin–orbit coupling as explained in our earlier work on PbTe [26] by doubling the Hamiltonian to a 16×16 matrix with two additional parameters λ_{Pb} and $\lambda_{S(Se,Te)}$ to describe the spin–orbit interaction. We use values for λ_{Pb} and $\lambda_{S(Se,Te)}$ taken from Herman's atomic calculations [27] as given in Table 1.

The pressure dependence of the energy gap in these semiconductors was calculated using the following relations:

$$\left(\frac{\partial E_g}{\partial P} \right)_T = \left(\frac{\partial E_g}{\partial V} \right)_T \left(\frac{\partial V}{\partial P} \right)_T = -\frac{V_0}{B_0} \left(\frac{\partial E_g}{\partial V} \right)_T \tag{4}$$

The value of $(\partial E_g/\partial V)_T$ was obtained directly from the energy gap versus volume calculations, and the value of $(\partial V/\partial P)_T$ was obtained from the compressibility relationship:

$$k = \frac{1}{B_0} = -\frac{1}{V_0} \left(\frac{\partial V}{\partial P} \right)_T \tag{5}$$

where V_0 is the equilibrium volume and B_0 is the bulk modulus at the equilibrium volume.

Table 1
SK parameters, orthogonal 3-center, B1 structure fit to LAPW results within the GGA (On the left side column, we show the notation used in Ref. [26])

		PbS	PbSe	PbTe
$s, s(000)$	A–A	−0.18143	−0.28645	−0.26910
$x, x(000)$	A–A	0.54829	0.49088	0.47971
$s, s(110)$	A–A	0.00507	−0.01843	−0.01442
$s, x(110)$	A–A	0.01409	0.02049	0.01604
$x, x(110)$	A–A	0.00932	0.01172	0.00826
$x, x(011)$	A–A	−0.00746	−0.00489	−0.00286
$x, y(110)$	A–A	0.02250	0.02478	0.01592
$s, s(200)$	A–A	0.00790	−0.00173	−0.00152
$s, x(200)$	A–A	−0.02675	−0.01094	−0.00930
$x, x(200)$	A–A	0.04870	0.03984	0.03411
$y, y(200)$	A–A	0.00512	0.00257	0.00204
$s, s(000)$	B–B	−0.45728	−0.38841	−0.26815
$s, s(110)$	B–B	−0.00780	0.01562	0.01292
$s, x(110)$	B–B	0.01509	0.00659	0.00525
$x, x(000)$	B–B	0.23463	0.28056	0.32684
$x, x(110)$	B–B	0.00634	−0.00229	−0.00470
$x, x(011)$	B–B	−0.00091	0.00342	0.00531
$x, y(110)$	B–B	−0.00607	−0.00802	−0.00484
$s, s(200)$	B–B	−0.01202	−0.00390	−0.00156
$s, x(200)$	B–B	−0.01801	0.00068	0.00145
$x, x(200)$	B–B	−0.02463	−0.01141	−0.00721
$y, y(200)$	B–B	0.00151	0.00290	0.00370
$s, s(100)$	A–B	−0.00849	−0.04393	−0.03351
$s, x(100)$	A–B	−0.04720	−0.01674	−0.01420
$x, s(100)$	A–B	−0.09909	−0.11069	−0.09328
$x, x(100)$	A–B	−0.09429	−0.12221	−0.12170
$y, y(100)$	A–B	0.02275	0.03094	0.03415
$s, s(111)$	A–B	−0.00016	0.00459	0.00371
$x, s(111)$	A–B	−0.00066	0.00437	0.00416
$s, x(111)$	A–B	0.00027	0.00351	0.00539
$x, x(111)$	A–B	0.00074	−0.00072	−0.00134
$x, y(111)$	A–B	0.00345	0.00198	0.00077
λ_{Pb}		0.03119	0.03119	0.03119
$\lambda_{S(Se,Te)}$		0.00235	0.01026	0.02058

3. Results

The total energy of the lead chalcogenides (PbS, PbSe, PbTe) was calculated as a function of the lattice constant in the B1 (NaCl), B2 (CsCl) and B3 (ZnS) structures using the LAPW method in both the LDA and GGA forms of exchange and correlation. The volume dependence of the total energy using the GGA results is presented in Fig. 1 with the corresponding energy curve produced from the Birch fit [19]. The equilibrium volume, bulk moduli, and the pressure derivative of the bulk modulus, along with experimental measurements [28,29], theoretical values [2], and our LDA and GGA calculated values are listed in Table 2 for the rock salt phase (NaCl). The lattice constants from our LDA calculations are 1–2% smaller than the experimental values, while the GGA results are 1–2% larger. From these data, we also find that the lattice constant of these semiconductors increases as the atomic number of the chalcogen atom increases. The equilibrium lattice constants determined from our LDA calculations are in good agreement with those calculated by Wei and Zunger [2]. These theoretical LAPW values are nearly independent of the type of parametrization used in LDA. We used the Hedin–Lundqvist parametrization [18], while Wei–Zunger used the Ceperley–Alder form as parametrized by Perdew and Zunger [30]. However, both forms of LDA disagree with experiments [31] when it comes to the mechanical properties. Our calculated LDA values of the bulk moduli agree well with Wei and Zunger, but both are larger than the experimental value. Meanwhile, the GGA predicts bulk moduli in very good agreement with experiment for PbS and PbTe. In the case of PbSe, our GGA value of the bulk modulus is found to be 10% smaller than the experimental value, while the LDA result is larger than experiment by 8%.

In addition, we also report the equilibrium lattice

Table 2
Summary of experimental, Wei and Zunger and our calculations for PbS, PbSe, and PbTe (a_{eq}, B, and B' are lattice constant, bulk modulus, and its pressure derivatives, respectively, in the NaCl (B1) structure)

	Calc. (present results)		Calc. (Wei–Zunger) (Ref. [2])	Expt. (Landolt–Bornstein) (Ref. [28])
	GGA	LDA		
PbS				
a_{eq} (Å)	6.012	5.860	5.906	5.929
B (Mbar)	0.533	0.648	0.663	0.529
B'	4.637	4.291	4.38	
PbSe				
a_{eq} (Å)	6.196	6.053	6.098	6.117
B (Mbar)	0.491	0.583	0.608	0.541
B'	4.425	4.464	4.56	
PbTe				
a_{eq} (Å)	6.565	6.370	6.44	6.462
B (Mbar)	0.414	0.514	0.517	0.398
B'	3.352	4.080	4.52	

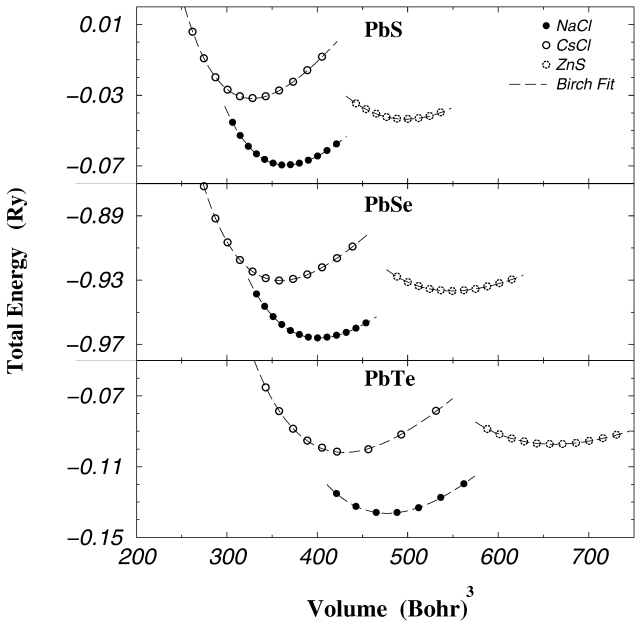

Fig. 1. Energy versus volume for the B1 (NaCl), B2 (CsCl) and B3 (ZnS) structures of the compounds PbS, PbSe, and PbTe. The filled and open circles represent the LAPW calculated energies within the GGA while the dashed lines are the fits to the Birch equation of state.

Table 3
Summary of our calculations for PbS, PbSe, and PbTe in the CsCl (B2) and ZnS (B3) structures (a_{eq}, B, and B' are lattice constant, bulk modulus, and its pressure derivatives, respectively)

	ZnS (B3) GGA	CsCl (B2)	
		GGA	LDA
PbS			
a_{eq} (Å)	6.657	3.649	3.548
B (Mbar)	0.392	0.558	0.698
B'	1.790	4.465	4.548
PbSe			
a_{eq} (Å)	6.876	3.763	3.672
B (Mbar)	0.320	0.515	0.628
B'	4.449	4.715	4.500
PbTe			
a_{eq} (Å)	7.320	3.997	3.879
B (Mbar)	0.254	0.409	0.503
B'	4.229	3.801	4.900

constant, the bulk modulus and its pressure derivative for the CsCl (B2) and ZnS (B3) structures in Table 3. We note, for the B2 structure, that the GGA lattice constants are larger than the LDA ones. Since we have neither theoretical nor experimental values to compare with, we leave these results as a reference for future investigation.

To study the stability of these compounds in the NaCl (B1) and CsCl (B2) structure, we have calculated the elastic constants at the equilibrium lattice constants and compare our results to the stability criteria in Eq. (3). We have found that in both structures these criteria are satisfied. The calculated and experimental values for the NaCl structure are listed in Table 4. From these results, we conclude that these compounds are stable against elastic deformation in the NaCl structure. Our calculations in the CsCl structure (not included in Table 4) also show stability against elastic deformation. Actual stability (or metastability in the case of CsCl) can only be determined by studying the phonon spectrum, which we do not calculate here. Comparing our theoretical values for the elastic constants to experiment, we find that the values of C_{11} using GGA to be in better

Table 4
Elastic constants of lead chalcogenides in the NaCl (B1) structure

	C_{11} (Mbar)			C_{12} (Mbar)			C_{44} (Mbar)		
	LDA	GGA	Expt. Ref. [28]	LDA	GGA	Expt. Ref. [28]	LDA	GGA	Expt. Ref. [28]
PbS	1.720	1.360	1.240	0.111	0.119	0.330	0.201	0.201	0.230
PbSe	1.595	1.208	1.237	0.078	0.089	0.193	0.180	0.172	0.159
PbTe	1.442	1.157	1.053	0.015	0.042	0.070	0.157	0.143	0.132

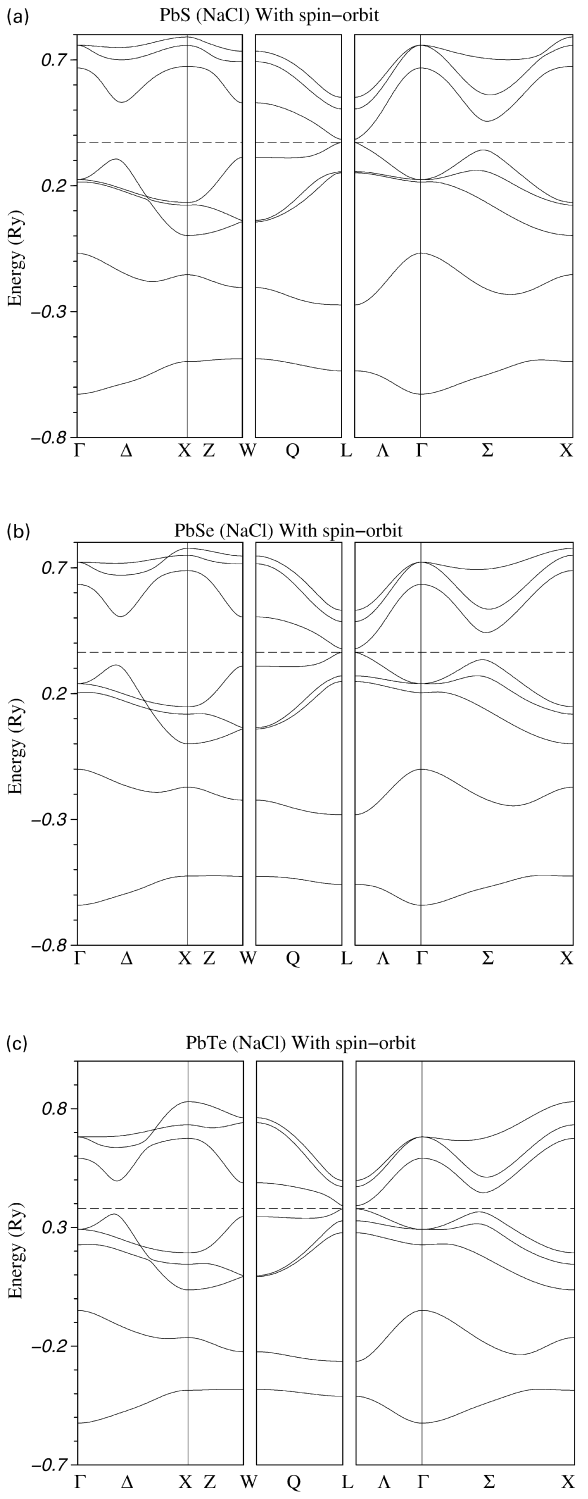

Fig. 2. The band structure along the symmetry lines of the BZ at the experimental lattice constant, (a) PbS, $a_{eq} = 5.929$ Å, (b) PbSe, $a_{eq} = 6.117$ Å, and (c) PbTe, $a_{eq} = 6.462$ Å. These bands were calculated within the SK formalism of TB including spin–orbit effects. The position of the Fermi level is shown by the dashed vertical line.

agreement with experiment than those based on LDA, while the values of C_{12} disagree with experiment in both approximations. However, the values of C_{44} are in good agreement with the experiment in both approximations.

As shown in Table 2, the equilibrium lattice constant is underestimated in the LDA and overestimated in the GGA. For this reason, we chose to calculate the band structure at the experimental lattice constant, since we found significant variation of the gap with lattice constant. Both LDA and GGA accurately locate the band gap at the L point of the Brillouin zone. For the width of the band gap, the LDA gives good agreement with experiment for PbS and PbSe and surprisingly overestimates the value for PbTe. Astonishingly, the GGA overestimates the gap for all three compounds as shown in Table 5. Since we have ignored the effect of spin–orbit coupling in these calculations, a significant contribution when heavy elements like lead (Pb) are present, we conclude that the LDA/GGA versus experiment comparison is inconclusive without spin–orbit. To test this, we include spin–orbit interactions by use of a TB parametrization.

In Fig. 2 the energy bands at the experimental lattice constants are obtained from the SK approach which also includes the spin–orbit coupling as described in Section 2. For each compound the first five bands of the band structure constitute the valence bands that accommodate the 10 electrons arising from the four s^2p^2 valence electrons of Pb and the six s^2p^4 valence electrons of the chalcogens (Te, Se, S). The next set of bands represents the conduction bands, which are separated from the valence bands by the gap described above. We note near the gap splitting of bands at the high symmetry points. The general features of the band structures shown in Fig. 2 are very similar with small differences in the various band widths.

In Table 5, we also list our SK values for the gap, including the spin–orbit interaction. We note that while in the LDA–SK the agreement with experiment has deteriorated, the GGA–SK values for the gap are in very good agreement with experiment. Although the LDA without spin–orbit gives fortuitously better agreement with the measured gap than the GGA with spin–orbit for the PbS and PbSe, we believe that the most accurate calculation for these materials should include the spin–orbit effects.

Our calculated band structures are in good agreement with those of Wei and Zunger, in terms of the overall ordering of the bands. In their LDA calculations Wei–Zunger had to adjust the gap by adding a constant potential to the conduction band states so that they can reproduce the experimental value exactly. In our SK approach, we can make an equivalent adjustment by varying the spin–orbit parameter λ_{Pb}. We find that values of $\lambda_{Pb} = 0.0552$, 0.0341, 0.0311 Ry for PbS, PbSe and PbTe, respectively, give the exact value of the width of the gap.

We also report, in Table 5, the pressure dependence of the energy gap for the lead chalcogenide semiconductors, using the LAPW method within the GGA approximation. This

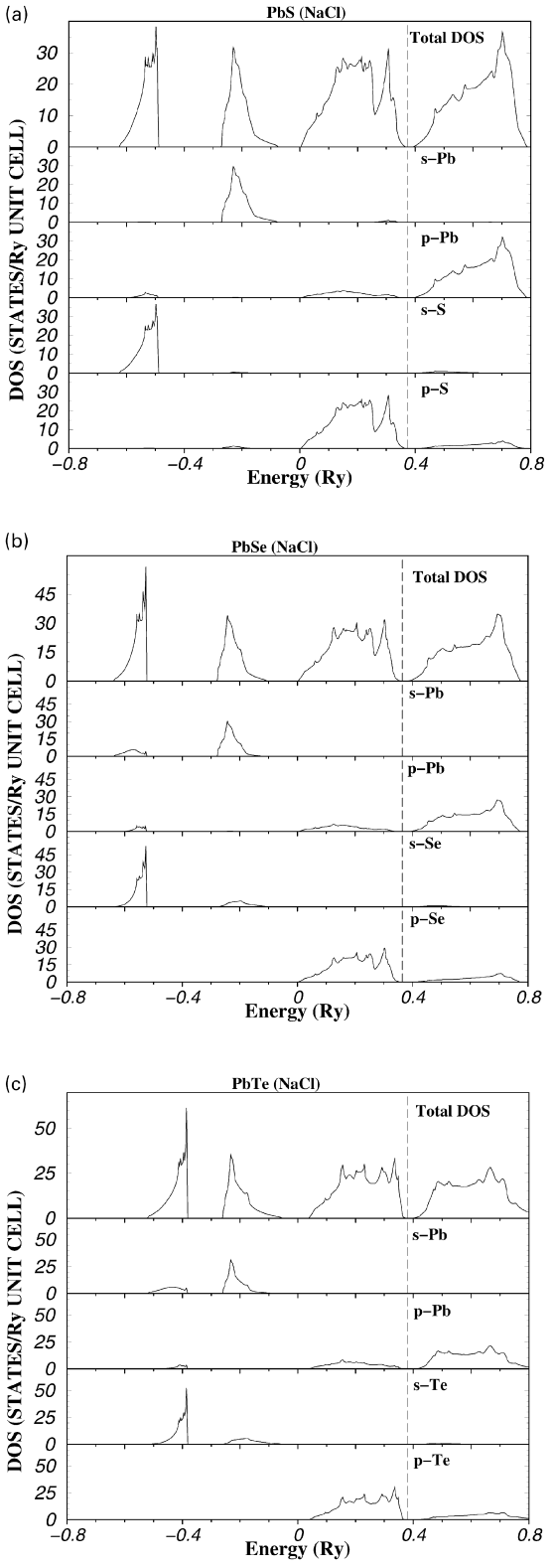

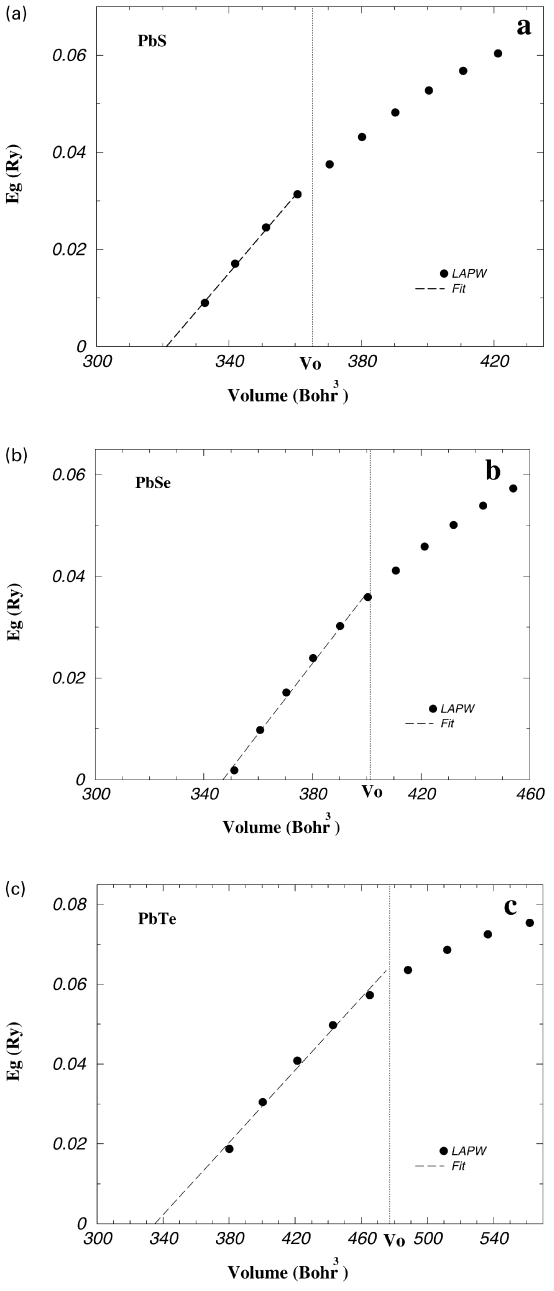

Fig. 4. The calculated volume dependence of the energy gap in the NaCl (B1) structure: (a) PbS, (b) PbSe, and (c) PbTe. The pressure coefficient is determined in the linear region, i.e. below the equilibrium volume V_0.

Fig. 3. Total and angular momentum-decomposed densities of states in the NaCl (B1) at the experimental lattice constant, derived from our SK Hamiltonian. (a) PbS, $a_{eq} = 5.929$ Å, (b) PbSe, $a_{eq} = 6.117$ Å, and (c) PbTe, $a_{eq} = 6.462$ Å. The position of the Fermi level is shown by the dashed vertical line. For each compound, the lower panels show the partial density of states at each atom site, decomposed by the angular momentum of the state.

Table 5
The energy gap values at L and Γ for PbS, PbSe, and PbTe in the NaCl (B1) structure at the experimental lattice constant

	Expt. Ref. [28]	LDA	GGA	SK fit (spin–orbit)	
				LDA	GGA
PbS					
$E_g(L)$ (eV)	0.290	0.220	0.340	0.026	0.187
$E_g(\Gamma)$ (eV)		7.223	7.290	6.116	6.031
$dE_g(L)/dP$ (eV/Mbar)	−9.100		−7.450		
PbSe					
$E_g(L)$ (eV)	0.170	0.170	0.380	0.110	0.214
$E_g(\Gamma)$ (eV)		6.466	6.601	5.229	5.367
$dE_g(L)/dP$ (eV/Mbar)	−9.100		−7.691		
PbTe					
$E_g(L)$ (eV)	0.19	0.645	0.737	0.087	0.188
$E_g(\Gamma)$ (eV)		5.320	5.377	3.956	4.072
$dE_g(L)/dP$ (eV/Mbar)	−7.500		−5.871		

value is deduced from Eq. (4), and as shown in Fig. 4 the volume dependence of the energy gap is determined from the slope of a linear region below the equilibrium volume. Our GGA calculation results in dE/dP values which are in better agreement with experiment than the Wei–Zunger LDA calculations. In addition, we have found that there is a metallic phase transition at small volumes as shown in Fig. 4. According to our LAPW–GGA calculations the pressures of these transitions to a metallic state are 84.73, 94.39 and 117.15 Mbar for PbS, PbSe and PbTe, respectively. We have plotted the energy bands below these pressures and found that the gap at L closes completely and the bands cross. In the interest of space we do not present another figure. The fact that the computed pressure coefficient is in reasonable agreement with experiment indicates that the spin–orbit effect would be uniform as a function of volume and therefore we have not calculated dE/dP for the SK results.

We can identify the character of the band states for these compounds by computing the total density of states and the site decomposed DOS. In Fig. 3, it is shown that for each compound the bands just below the Fermi level (E_F) are predominately p states of the chalcogen with only a small contribution from p-Pb. The lowest band has exclusively chalcogen atom s character, while the next band has the s character of Lead and lies far below the gap. Above the gap the dominant component is of p-Pb character.

Finally, in our LDA and GGA calculations of these compounds in the CsCl structure we found no gap at any lattice constant. As an example the band structure of the compound PbS using the GGA is shown in Fig. 5. Our results do not agree with transmittance and reflectance

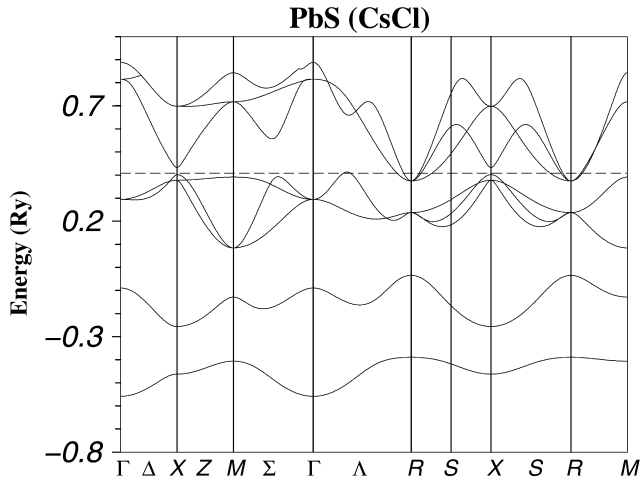

Fig. 5. The PbS band structure along the symmetry lines of the BZ in the CsCl (B2) structure at the equilibrium lattice constant. These bands were calculated using the LAPW method within the GGA approximation.

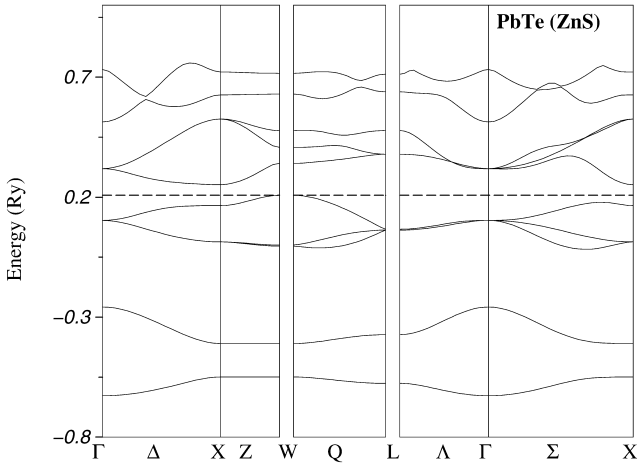

Fig. 6. The PbTe band structure along the symmetry lines of the BZ in the ZnS (B3) structure at the equilibrium lattice constant $a_{eq} = 7.320$ Å. These bands were calculated using the LAPW method within GGA approximation.

spectra measurements performed on PbTe by Baleva and Mateeva [32] who found a gap of 0.21 eV. We do find a band gap when these calculations were performed in the ZnS structure. We show as example in Fig. 6, the ZnS band structure of PbTe. An indirect band gap is found between the symmetry points *X* and *W*.

4. Conclusions

We have employed the LAPW method with both the LDA and GGA forms of exchange and correlation to determine the electronic band structure and elastic constants of the lead chalcogenide compounds (PbS, PbSe, PbTe). The results from both approximations show that the equilibrium lattice constants are in good agreement with experiment and previous theoretical studies [2]. In general, our calculated GGA values of the mechanical properties of these compounds in the NaCl (B1) structure gives the best agreement with experiment. We constructed an orthogonal sp^3 basis SK Hamiltonian, including the spin–orbit coupling and fitted both our LDA and GGA results using the atomic values of the spin–orbit parameters. We found that the SK/GGA give an energy gap in good agreement with experiment. In addition, we found that these compounds may have metastable structures as metals in the CsCl structure and as semiconductors with an indirect band gap in the ZnS structure.

Acknowledgements

This research was supported by the US Office of Naval Research and the Common High Performance Computing Software Initiative (CHSSI) of the United States Department of Defence High Performance Computing Modernization Program (HPCMP). This work was also supported in part by a grant of HPC time from the DoD HPC Center, for computations on the IBM SP2 and SGI Origin at the Aeronautical Systems Center, Wright-Patterson Air Force Base, Dayton, OH.

References

[1] H.K. Henisch (Ed.), Semi-Conducting Materials Butterworth Scientific Publications, London, 1951, p. 78 See also p. 87 and 198.
[2] S. Wei, A. Zunger, Phys. Rev. B 55 (1997) 13605.
[3] O.K. Andersen, Phys. Rev. B 12 (1975) 3060.
[4] D. Singh, H. Krakauer, C.S. Wang, Phys. Rev. B 34 (1986) 8391.
[5] W. Kohn, L.J. Sham, Phys. Rev. 140 (1965) A1133.
[6] D.L. Mitchell, R.F. Wallis, Phys. Rev. 151 (1966) 581.
[7] J.B. Conklin Jr., L.E. Johnson, G.W. Pratt, Phys. Rev. 137 (1965) A1282.
[8] P.T. Bailey, Phys. Rev. 170 (1968) 723.
[9] H. Overhof, U. Rossler, Phys. Stat. Sol. 37 (1970) 691.
[10] F. Herman, R.L. Kortum, I.B. Ortenburger, J.P. Van Dyke, J. Phys. (Paris) 29 (1968) c4–c62.
[11] G. Martinez, M. Schluter, M.L. Cohen, Phys. Rev. B 11 (1975) 651.
[12] G. Martinez, M. Schluter, M.L. Cohen, Phys. Rev. B 11 (1975) 660.
[13] P.J. Lin, K. Kleinman, Phys. Rev. 142 (1966) 478.
[14] R.L. Bernick, L. Kleinman, Solid State Commun. 8 (1970) 569.
[15] Y.W. Tung, M.L. Cohen, Phys. Rev. 180 (1969) 823.
[16] J.P. Perdew, J.A. Chevary, S.H. Vosko, K.A. Jackson, M.R. Pederson, D.J. Singh, C. Fiolhais, Phys. Rev. B 46 (1992) 6671.
[17] D.R. Koelling, B.N. Harmon, J. Phys. C 10 (1977) 3107.
[18] L. Hedin, B.I. Lundqvist, J. Phys. C 4 (1971) 2064.
[19] F. Birch, J. Geophys. Res. 83 (1978) 1257.
[20] M.J. Mehl, J.E. Osburn, D.A. Papaconstantopoulos, B.M. Klein, Phys. Rev. B 41 (1990) 10311.

[21] M. Mehl, B.M. Klein, D.A. Papaconstantopoulos, in: J.H. Westbrook, R.L. Fleischer (Eds.), Principles, Intermetallic Compounds, vol. 1, Wiley, New York, 1995 Chapter 9.
[22] M. Born, K. Huang, Dynamical Theory of Crystal Lattices, Clarendon, Oxford, 1956.
[23] J. Wang, S. Yip, Phys. Rev. Lett. 71 (1993) 4182.
[24] J.C. Slater, G.F. Koster, Phys. Rev. 94 (1954) 1498.
[25] D.A. Papaconstantopoulos, Handbook of Electronic Structure of Elemental Solids, Plenum, New York, 1986.
[26] M. Lach-hab, D.A. Papaconstantopoulos, M.J. Mehl, J. Phys. Chem. Solids 61 (2000) 1639.
[27] F. Herman, S. Skillman, Atomic Structure Calculations, Prentice-Hall, Englewood Cliffs, NJ, 1963.
[28] O. Madelung, M. Schulz, H. Weiss (Eds.), Numerical Data and Functional Relationships in Science and Technology Landolt–Bornstei, New Series, vol. 17, Springer, Berlin, 1983.
[29] G. Nimtz, B. Schlicht, Narrow-Gap Semiconductors, Springer, New York, 1985.
[30] J.P. Perdew, A. Zunger, Phys. Rev. B 23 (1981) 5048.
[31] S. Rabii, Phys. Rev. 167 (1968) 801.
[32] M. Baleva, E. Mateeva, Phys. Rev. B 50 (1994) 8893.